C2012-0001442

NACE INTERNATIONAL CORROSION 2012 CONFERENCE & EXPO

EVALUATION OF BRISTLE BLASTING PROCESS FOR SURFACE PREPARATION OF SHIP-CONSTRUCTION STEEL

Professor Robert J. Stango, Ph.D., P.E. (robert.stango@mu.edu),
and Ellen Kargol, Graduate Research Assistant
Mechanical Engineering Department
1515 West Wisconsin Avenue
Marquette University
Milwaukee, WI 53233 USA

ABSTRACT

Surface preparation of ship-construction steel is an important concern throughout the ship building and refurbishing community. To this end, blast-cleaning processes are routinely used for corrosion removal and surface preparation prior to the application of protective paints and coatings. However, blast cleaning processes are cumbersome and inevitably require special equipment, containment systems, and subsequent clean-up due to the widespread environmental contamination that is inherent of the process. At the same time, alternate methods of corrosion removal such as needle gun/scaler tools are known to cause irreversible hand/wrist injury due to excessive exposure to vibration. Consequently, there is a strong need to develop alternative surface preparation processes that forego the expense, environmental contamination, and risk of injury that is commonly associated with existing cleaning and surface preparation processes.

In this technical paper, an alternative surface preparation process termed bristle blasting is presented, which simultaneously removes corrosion and generates a surface profile that is equivalent to commercial grit blasting processes. Specifically, performance of the bristle blasting process is examined within the context of treating common structural steel ABS-A, which is used in the ship building community. Results are reported that summarize the most recent findings for cleanliness, texture, and material removal performance that can be achieved for base metal materials. In addition, surface and subsurface modification of the bristle blasted region is examined in order to help assess the plastic deformation and residual stress state that is imparted to the steel during the surface preparation process. These results, collectively, are used for assessing the suitability of introducing bristle blasting tool technology for cleaning/texturing steels that are peculiar to this industry.

INTRODUCTION AND BACKGROUND

Periodic corrosion removal and reapplication of paint and coating to ship-construction steel is an essential part of the ship building and refurbishing community. Although grit blasting is the most widely used method for preparing steel surfaces, maintenance engineers are constantly searching for alternative surface treatment processes that can avoid many of the difficulties and inherent dangers of grit blasting, which is neither environmentally nor user friendly. A new process termed bristle blasting, which will be discussed in this paper, utilizes a rotary power tool for simultaneously removing corrosion and generating an anchor profile. While the bristle blasting tool physically resembles wire brushes, the wire bristles are designed to strike the target surface and immediately rebound as the spindle rotates. That is, the bristle blasting tool is dynamically tuned such that each bristle tip rebounds upon impact, thereby resulting in impact craters that are similar to the surface profile created by grit-blasting processes. This rebound is an occurrence that is unique to the bristle blasting tool. Although the tool is commercially available, findings are still being made concerning the performance of the bristle blaster tool in treating common structural steel ABS-A, which is used in the ship building community. Performance of the bristle blasting process is examined for cleanliness, material removal, and texture/anchor profile. In addition to these findings, the theoretical impulsive load will be evaluated through an analysis of the impact mechanics of the problem, thereby providing insight into the surface deformation and residual stresses that are generated during the surface treatment process. Finally, the paper will report recent findings regarding the surface and subsurface residual stress state that arises due to bristle blasting process.

BRISTLE BLASTING PROCESS

Equipment and Principle of Operation

Essential components of the bristle blasting system are shown in Figure 1a, and consist of the power tool main body and spindle, which drives the bristle blasting tool/hub assembly. Additional details concerning the tool construction appear in Figure 1b, whereby bristles are secured to- and protrude through- a flexible belt/hub assembly. During operation, the bristle

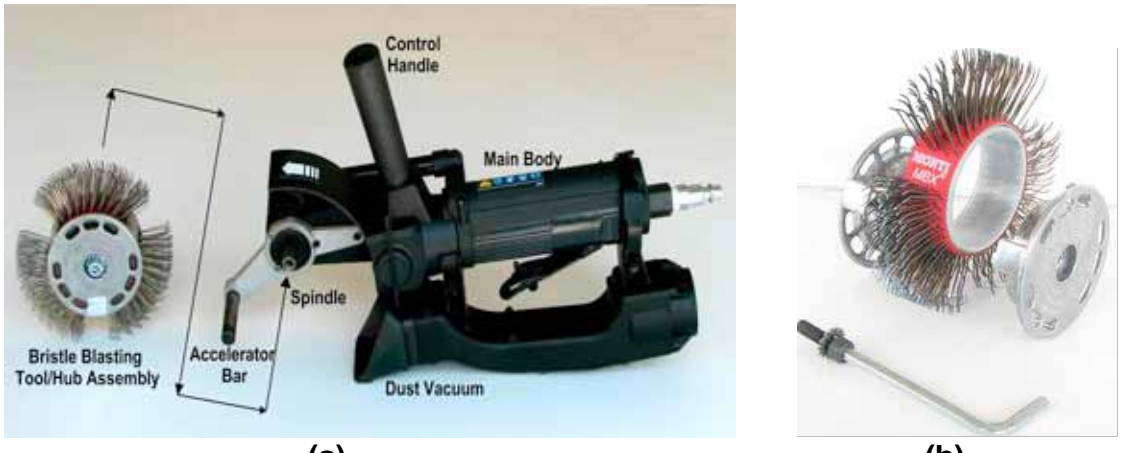

Figure 1. (a) Components of bristle blasting power tool, including tool/hub assembly and power tool body with pneumatically driven spindle, and (b) Assembly view of bristle blasting tool along with attachment hubs

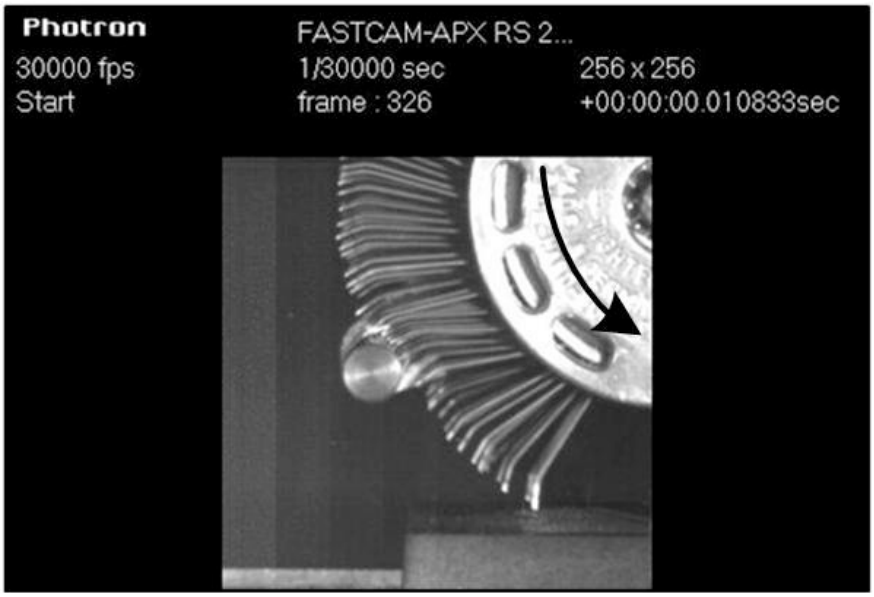

Figure 2. Photograph/cell taken from high speed digital camera illustrating bristle tips in contact with accelerator bar, and subsequent release/spring-back toward workpart surface.

tips strike the accelerator bar and retract, thereby storing energy which is subsequently released during spring-back, as shown in Figure 2. This concept is further depicted in the schematic diagram shown in Figure 3, whereby forward-bent bristle tips repeatedly strike the target surface and subsequently rebound after impact. The impact and rebound event has been captured via high-speed digital camera, and is shown in seven consecutive frames in Figure 4. Frame 1 illustrates the approach (pre-impact) of the bristle tip, whereas frame 2

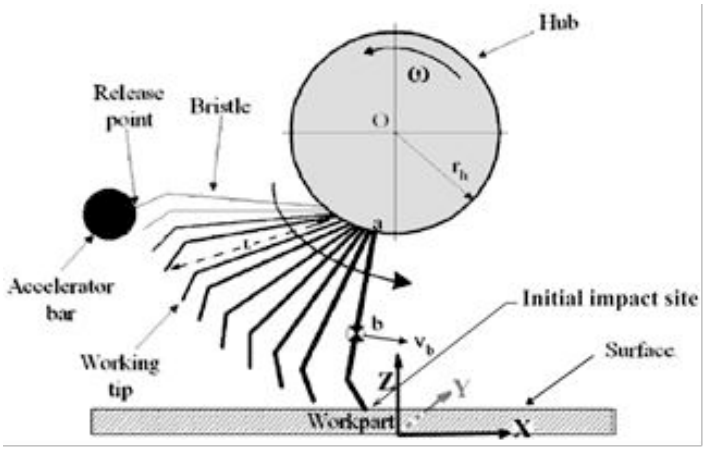

Figure 3 Schematic of wire bristle motion during bristle blasting process, and coordinate system used for rectifying tool force components exerted onto the workpart surface.

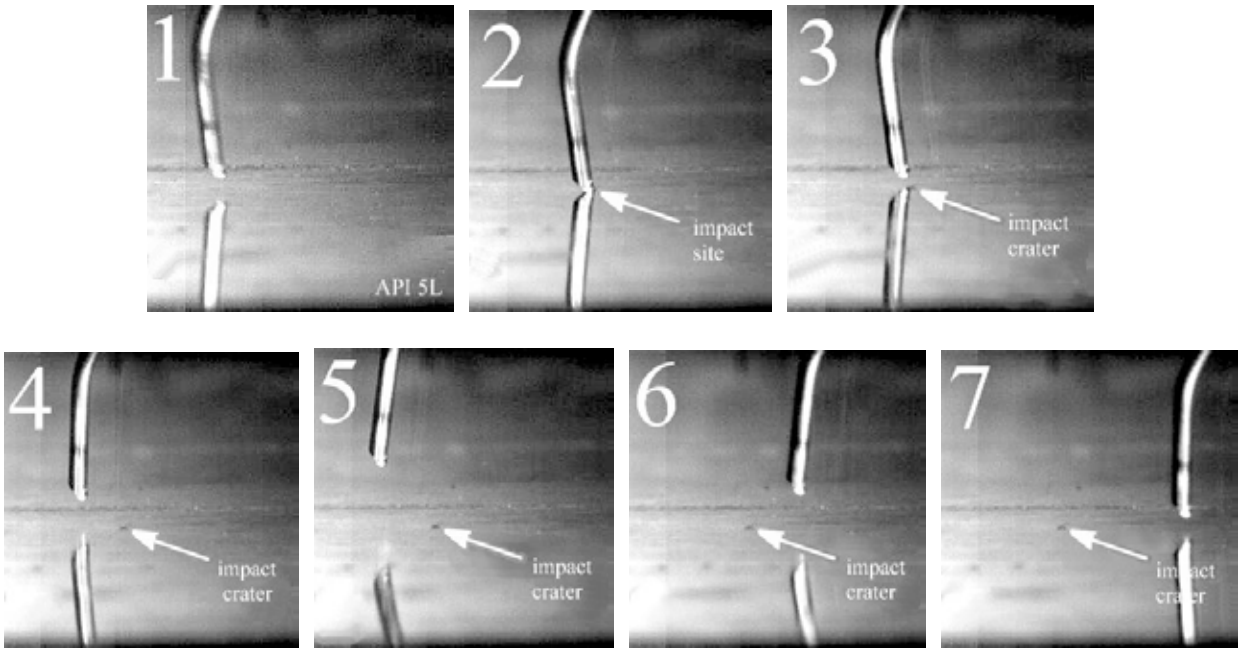

Figure 4. Seven consecutive frames captured from a high-speed digital camera depicting the approach of the bristle tip (Frame [1]); impact (Frame [2]); retraction (Frames [3], [4], and [5]); and continued movement of the bristle tip away from the contact region (Frames [6] and [7]).

shows the instant at which contact is made with the workpart surface. Frames 3 through 7 depict the position of the bristle tip during various stages of post-impact, and demonstrate retraction of the bristle tip from the surface (frames 3, 4, and 5), and subsequent forward movement (frames 6 and 7) as the bristle tip retreats to an equilibrium position.

Further details of the impact crater that was formed during frame 2 are shown using the scanning electron microscope (SEM) in Figure 5a, whereby the displaced material has the appearance of *shoveling*, which is a direct consequence of low incident angle contact that has been made at the interface of the bristle tip and target surface. The overall texture that is characteristic of repetitive bristle impact is shown in Figure 5b, and has a granular appearance similar to that formed during grit blasting processes. At the somewhat higher magnification shown in Figure 5c (see enlargement of region depicted by inset arrow), a series of superposed impact craters are clearly visible.

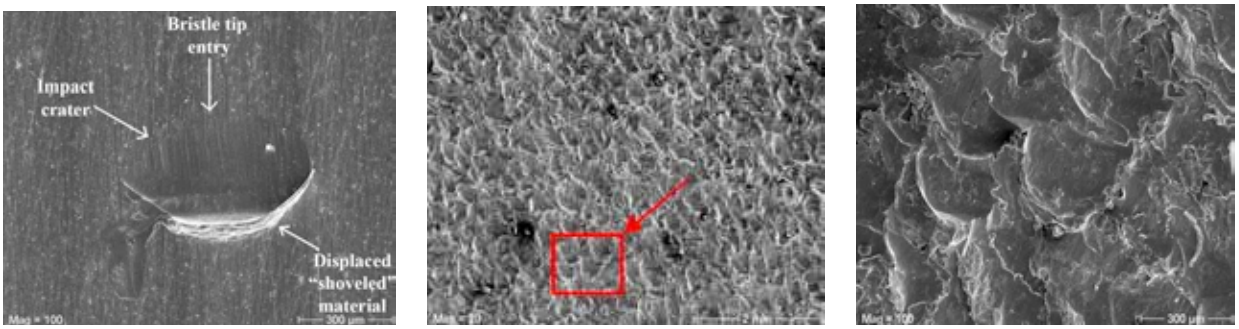

Figure 5. (a)Typical impact craters generated by bristle tips during contact event shown in frame 2; (b) Scanning electron micrographs of the bristle blast treated surface shown at 20x; and (c) higher resolution scanning electron micrograph (100x) of region indicted by inset arrow shown in Figure (4b).

Implementation of Bristle Blasting Process

A standard procedure has been proposed elsewhere (see references [1-3]) for successfully implementing the bristle blasting process, and is repeated in this section in order to help acclimate readers with a methodology that is currently held as best practice.

All manual surface treatment processes require dexterity, visual acuity, and a basic understanding of key parameters that affect the performance of surface finishing equipment. Training and experience are, therefore, important factors that enable users to develop skills that are needed for a successful outcome. The skill-sets that are essential for successful application of the bristle blasting process are quite similar to those needed for other surface treatment processes, and include the following: 1) proper orientation of the tool in relation to the target surface, 2) control of tool force exerted onto the surface, and 3) the feed rate and direction of the tool during operation. In the following discussion, each of these user-based considerations is briefly discussed within the context of a common corrosion removal application.

Initializing the process cleaning parameters

Appropriate selection of the bristle blasting process parameters can be readily established by first, identifying a candidate surface that requires cleaning, and isolating a portion of the surface for initial cleaning/testing. In general, the face of the tool hub is oriented perpendicular to the treated surface during use, as shown in Figure 6. During corrosion removal, the bristle tips are brought into direct contact with the corroded surface using minimal applied force, and the rotating tool is gradually moved along the feed direction, that is, either to the left or right of the user (see Fig. 6a). Thus, the appropriate pressure and feed rate of the tool is obtained by

(a) **(b)** **(c)**

Figure 6. Recommended use of bristle blasting tool for corrosion removal. First, a horizontal row is prepared (Fig. 5(a)) using minimal applied force and steady feed rate. The process is then repeated by overlapping the second row (Fig. 5(b)) with the previous row that was cleaned. Finally, the entire surface is cleaned (Fig. 5(c)) by repeatedly overlapping each row with the previously cleaned region until full coverage is completed.

direct experimentation and by visually inspecting the trial-tested region to ensure that the desired cleaning standard/requirement is reached.

Method/pattern for continuous systematic cleaning

Having obtained the appropriate process parameters for corrosion removal, the user then identifies the region to be treated, and develops a simple plan for obtaining complete coverage. As shown in Fig. 6a, for example, the surface of a corroded steel component must be cleaned. The user, in turn, has elected to begin the corrosion removal process at the extreme left end of the component, and has applied the working surface of the tool along the

feed direction, i.e., from left to right. This procedure has resulted in a cleaned and textured horizontal *band* or *row*, which appears in Fig. 6a. Equally important, the user has started the cleaning operation along the top (uppermost) portion of the corroded surface, and will perform all subsequent cleaning by the use of overlapping bands that have their starting point *below* (under) the previously cleaned region. That is, correct use and *optimal cleaning/texturing performance* of the tool requires that each overlapping successive band is generated *beneath* the previously cleaned region/row. Therefore, as shown in Fig.6b, the user has correctly overlapped the previously cleaned region, and has generated/cleaned the next row by placing the working surface of the rotating tool directly below the initially prepared surface.

Completing the corrosion removal process

Corroded components can be completely cleaned by repeating the previously described procedure. Thus, as shown in Fig. 6c, the top surface of the corroded beam has been completely cleaned, and the user is ready to remove corrosion from any remaining surfaces. Finally, if any portion of the surface is identified where unsatisfactory cleaning has been obtained, the user can return to these locations for final "touch-up" cleaning, as needed.

Compilation of Tool Performance for ABS-A Steel

In this section, results are compiled and summarized for various aspects of bristle blasting tool performance that have been heretofore reported in the literature for ABS-A steel. This includes, for example, user-applied forces exerted onto the workpart surface, cleanliness, material removal performance, and the anchor profile/texture that one may expect during implementation.

User-applied force and workpart penetration

As shown in Figure 6a, the bristle blast power tool is operated by grasping both the control handle and the main body of the tool, and directly exerting the working surface of the tool against the contaminated surface. Consequently, direct coupling of the user/tool and workpart surface generates a force that characterizes the cleaning and material removal process. In this case, the force components F_x, F_y, and F_z [ref. Figure 3] associated with bristle blasting is reported in Figure 7 for two different levels of force exerted by the operator. The first plateau corresponds to ordinary use of the tool, and results in a mean operating force of approximately 13 N (3 lb), whereas the second plateau corresponds to heavy penetration of the tool, and

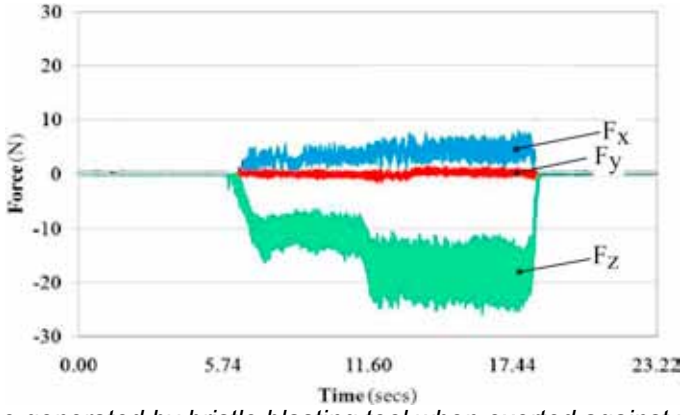

Figure 7 Measured force generated by bristle blasting tool when exerted against vertical steel surface during typical surface cleaning exercise. Two different levels of force exertion, namely, normal (first plateau) and heavy (second plateau) were used during the cleaning operation.

results in a mean operating force of approximately 20 N (4.5 lb). In general, increased penetration of the tool yields a corresponding increase in the (average) *normal impact force*, F_Z

applied by bristle tips to the workpart surface, whereas the in-plane shear force F_X shows minimal change. Finally, the out-of-plane force F_Y is negligible as expected, because alignment of the tool as shown in Figure 3 does not generate appreciable force in the lateral direction.

Cleanliness

Condition of an as-received flat panel is shown in Figure 8(a), and depicts uniform, severe corrosion [SSPC Condition Grade D (100% rust with pits)]. The lower portion of the panel was

(a) **(b)** **(c)**

Figure 8 (a) Initial corroded surface of as-received ABS-A specimen prior to cleaning (top) and after bristle blast cleaning (bottom), (b) Photograph depicting the severity of corrosion/pitting on the as-received surface, and (c) cleanliness of the bristle blasted surface after corrosion removal.

subsequently cleaned via bristle blasting, and indicates that the cleanliness level SP-5 (white metal blast cleaning) has been achieved. Detailed view of the pre-treated and post-treated surface is further illustrated in Figures 8(b), and 8(c), respectively.

Material removal

Material removal performance of the tool has been assessed by using the bristle blasting tool in conjunction with a 3-axis milling machine that accommodates precision placement of the tool during operation. Thus, the results reported in Figure 9 show the gram-weight extracted from the specimen by a new tool (i.e., as-received) when subjected to three different penetration depths, namely, 0.10 in., 0.15 in., and 0.20 in. These results indicate that deeper penetration (i.e., greater insertion of the tool) results in progressively greater material removal from the base metal.

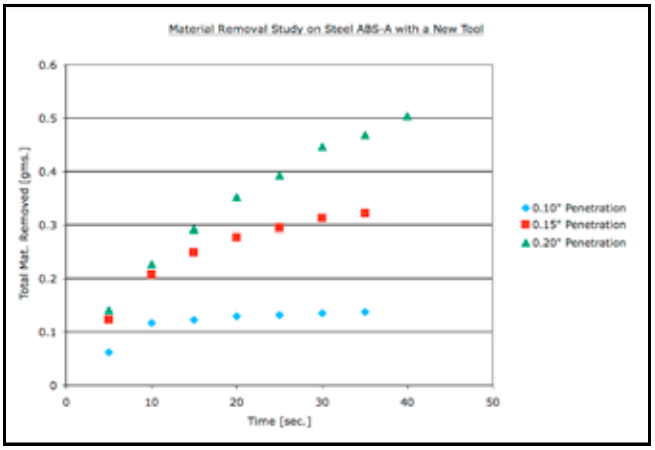

Figure 9 Material removal performance of new bristle blasting tool (i.e., as-received) when applied to ABS-A flat panel at three different penetration depths, 0.10 in., 0.15 in., and 0.20 in.

One may expect that repeated use of the tool will inevitably lead to progressive wear of bristle tips which, in turn, will be accompanied by reduced tool performance. Therefore, performance of the tool has been reassessed in Figure 10 for a tool that has been subjected to a continuous duty cycle of 25 minutes, and again in Figure 11 for a tool that has been

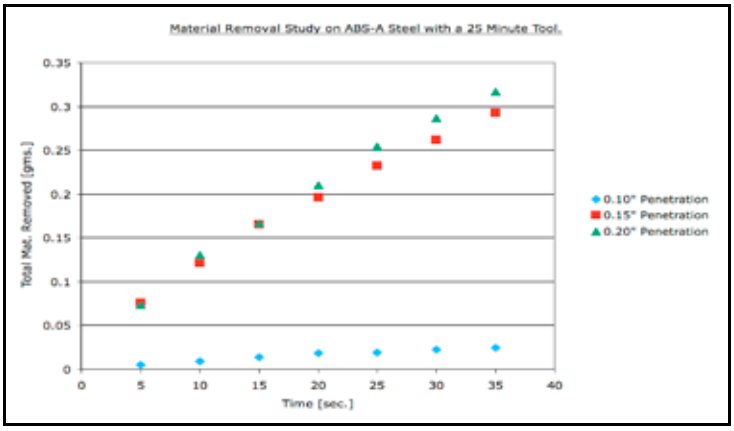

Figure 10 Material removal performance of aged blasting tool (i.e., 25 minute duty cycle acquired) when applied to ABS-A flat panel at three different penetration depths, 0.10 in., 0.15 in., and 0.20 in.

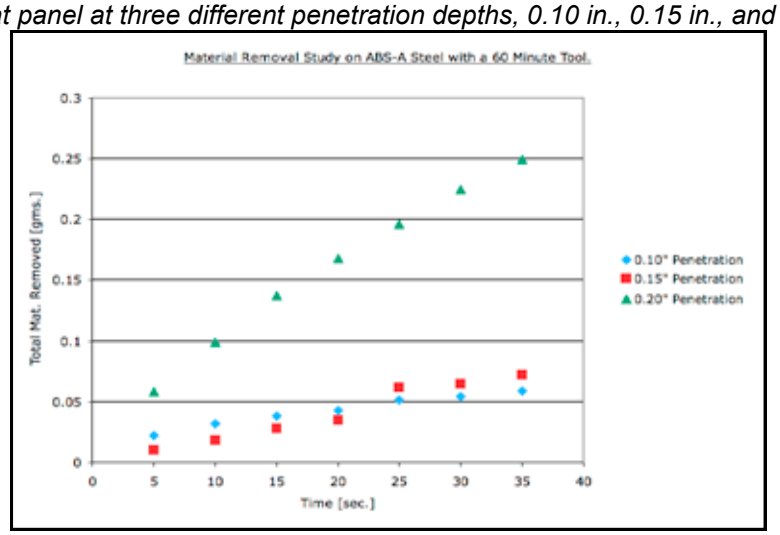

Figure 11 Material removal performance of aged blasting tool (i.e., 60 minute duty cycle acquired) when applied to ABS-A flat panel at three different penetration depths, 0.10 in., 0.15 in., and 0.20 in.

subjected to a continuous duty cycle of 60 minutes. Examination of these results indicates that in general, material removal performance is greatest at the deepest penetration depth. Also, these results show that as the tool ages, the material removal/extraction progressively declines.

Anchor profile/texture

In Figure 12, surface roughness parameter R_Z (microns) has been obtained using a Mitutoyo Surftest SJ 301 stylus surface roughness measurement instrument. The reported data represents the average of three separate measurements that were taken at random positions along the textured surface. These results indicate that the profile imparted to the surface progressively declines as the tools ages over a one hour duty cycle. Also, the profile obtained appears to be similar whether low (0.10 in.), medium (0.15 in.), or high (0.20 in.) penetration depth is applied to the tool.

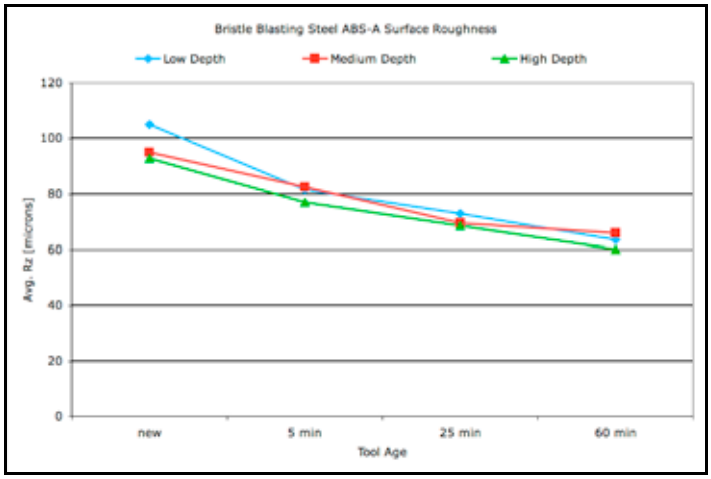

Figure 12 Roughness parameter Rz measured at low (0.10 in.), medium (0.15 in.), or high (0.20 in.) penetration depth as the tool progressively ages over a one hour duty cycle.

ELEMENTARY MODELING CONSIDERATIONS

Monofilament Behavior

Prior to developing a mechanics based model for evaluating bristle/workpart impact, it is helpful to examine the post-impact behavior of three bristle shapes shown in Figure 13, namely, a reverse-bent bristle (13a), straight bristle (13b) and forward-bent bristle (13c). In each case, the bristle is rotating in the counterclockwise direction at approximately 2,500 rpm,

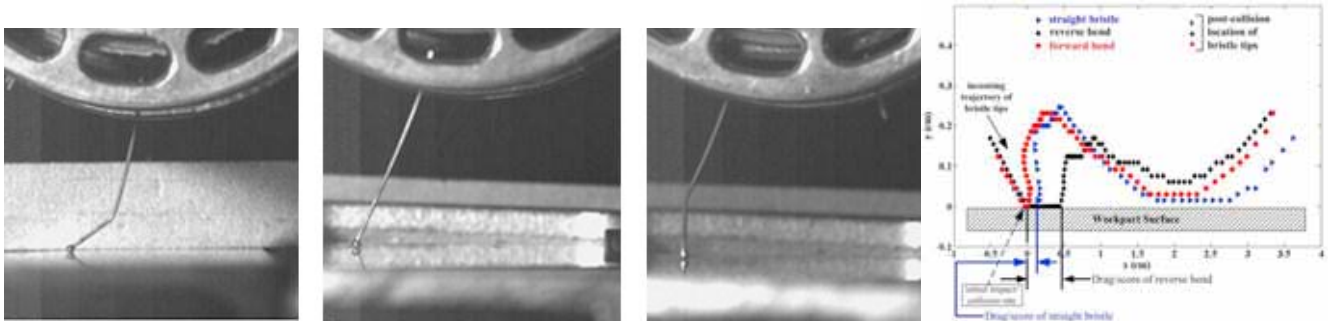

(a) **(b)** **(c)** **(d)**

Figure 13 Geometry of three differently configured rotating bristles, featuring 9a (reverse bent knee), 9b (straight without bend) and 9c (forward bent knee). Upon impact with the surface (bristle is moving from left to right), the bristle tip rebounds, and its location is precisely monitored via high-speed digital camera and shown in 9d.

and the precise position of the spherical tip (monitored via high-speed digital camera) is depicted in Figure 13d throughout the pre-and post-collision period. Careful examination of the bristle tip trajectory for all three cases shows that the initial impact of the bristle tip is followed by retraction/rebound from the surface, and is not accompanied by a secondary impact. The dynamic response of the forward-bent bristle is of greatest interest, and indicates that *no sliding motion* occurs between the tip/workpart surface throughout the duration of contact.

This filament geometry (i.e., forward bent knee) is similar to those that comprise the bristle blasting tool, and suggests that both impact and rebound have characteristics that are similar to rigid body collision mechanics. That is, impact and rebound of the bristle tip occurs only at an isolated point of contact, and is immediately followed by retraction/reversal of direction.

Dynamic properties of the forward-bent bristle are further examined in the time-lapse digital image shown in Figure 14, whereby the complete contact event is recorded in eleven (11) successive frames. That is, as the bristle rotates in a counterclockwise direction, (motion is from left-to right), the pre-contact geometry of the bristle is clearly visible in frames 1, 2, and 3. Upon contact (frame 4) the bristle tip strikes and subsequently rebounds from the surface (frame 5), while the body of the filament pivots about the point of attachment at the hub/belt. Throughout the post impact duration, the hub continues to rotate and the final trajectory of the bristle is shown in frames 6-11. Thus, the time-lapse image clearly indicates that contact and retraction of the bristle tip occurs only at an isolated point, and the bristle retains original shape throughout the pre- and post- collision process. Consequently, key elements of rigid body collision mechanics are retained, which suggests that formulation of the problem may be simplified, and need not examine bristle deformation and wave propagation through the body of the filament.

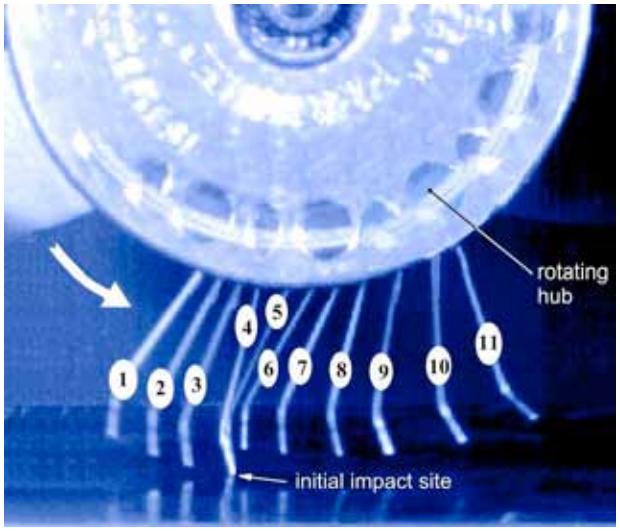

Figure 14 Successive frames of a single bristle taken from high-speed digital camera depicting the approach (frames 1, 2, and 3), contact/collision (frame 4), subsequent retraction (frame 5), and return to equilibrium position (frames 6-11) of bristle.

Theoretical Formulation of the Problem

Previous observations that were made regarding monofilament behavior and time-lapse imagery can provide a rational basis for invoking rigid body mechanics to evaluate the bristle/workpart collision process. In order to gain insight into the impulsive load that arises

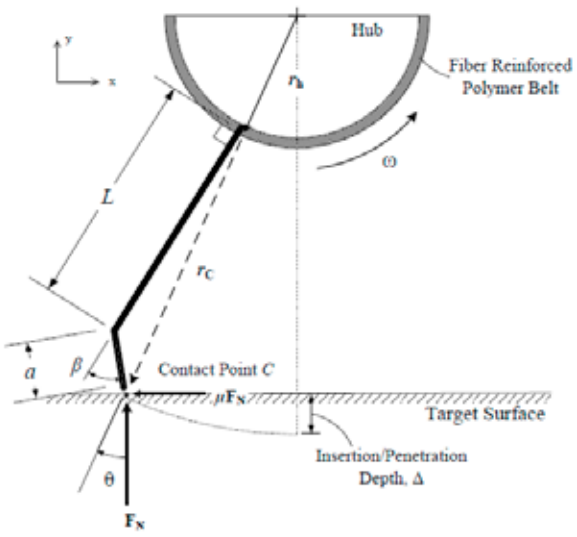

Figure 15 Idealized model/schematic of bristle in contact with rigid surface

during impact, essential features of the problem are shown in Figure 15. This idealization of bristle geometry forms a basis for an analyzing the dynamics of the bristle tool via generalized impulse and the equations of motion. That is, the behavior of a single bristle is examined in order to derive the impulsive load that the target surface undergoes during tool use. By using appropriate velocity constraints, the equations of motion in terms of generalized speeds can be obtained directly from kinetic energy and the differential of generalized impulse.

During tool operation, the kinetic energy *T* of a single bristle can be written as follows:

$$T = \frac{1}{2} M k_r^2 \dot{\theta}^2 = \frac{1}{2} M \dot{q}_1^{\,2} \qquad (1)$$

where *M* is the mass of a single bristle, k_r is the radius of gyration, and $\dot{\theta}$ is angular velocity. Additionally, the generalized speed $\dot{q}_1 \equiv k_r \dot{\theta}$. Further, the tip of the bristle, which impacts the target surface at contact point *C*, has a velocity defined by

$$\vec{v}_c = \vec{v}_0 + \vec{\omega} \times \vec{r}_c = -\frac{r_{cy} \dot{q}_1}{k_r} \hat{\imath} - \frac{r_{cx} \dot{q}_1}{k_r} \hat{\jmath} \qquad (2)$$

where $\vec{r}_c = r_{cx} \hat{\imath} + r_{cy} \hat{\jmath}$ is the vector from the hub to the contact point, ω is the angular velocity, and $\vec{v}_0$ is the velocity of the origin.

In addition to the previously defined kinetic energy and velocity of a bristle, the differential of generalized impulse $d\Pi_r$ can be defined for the system. By definition, the only forces that contribute to the differential of generalized impulse are generalized active forces $F_r = \sum \frac{d\vec{p}_j}{dt} \cdot \frac{\partial \vec{v}_j}{\partial \dot{q}_r}$ [4]. Therefore, the differential of generalized impulse is equal to

$$d\Pi_1 = \sum_{j=1}^{n} d\vec{p}_j \cdot \frac{\partial \vec{v}_j}{\partial \dot{q}_r} = \frac{r_y}{k_r} dp_x - \frac{r_x}{k_r} dp_y \qquad (3)$$

where the differential of impulse $d\vec{p}_j = dp_x \hat{\imath} + dp_y \hat{\jmath}$.

It has been shown that as the bristle impacts the target surface, the tip reverses in direction at impulse p_c. Therefore, due to friction at the contact point between the bristle tip and the

target surface, the differential of impulse $d\vec{p}_j$ must satisfy the Amontons-Coulomb law for friction at contact point *C* [5]. For this reason, before rebound (when $\vec{v}_c \cdot \hat{\imath} < 0$), $dp_x = \mu dp_y$, and during rebound (when $\vec{v}_c \cdot \hat{\imath} > 0$), $dp_x = -\mu dp_y$. The differential of the generalized impulse is thus

$$d\Pi_1 = \begin{cases} -k_r^{-1}\left(r_x - \mu r_y\right) dp & \vec{v}_c \cdot \hat{\imath} < 0 \\ -k_r^{-1}\left(r_x + \mu r_y\right) dp & \vec{v}_c \cdot \hat{\imath} > 0 \end{cases} \tag{4}$$

where $dp = dp_y$ is the normal impulse acting on the bristle and target surface.

Additionally, using the kinetic energy, a differential of generalized impulse, $d\Pi_r = d\frac{\partial T}{\partial \dot{q}_r}$, is equal to

$$d\Pi_1 = d\frac{\partial T}{\partial \dot{q}_1} = d(M\dot{q}_1) \tag{5}$$

Combining Equations (4) and (5), and integrating, the following generalized speed as a function of normal impulse is

$$\dot{q}_1(p) = \begin{cases} -(k_r M)^{-1}\left(r_x + \mu r_y\right) p + \dot{q}_1(0) & p < p_c \\ -(k_r M)^{-1}\left(r_x - \mu r_y\right)(p - p_c) & p_c < p < p_f \end{cases} \tag{6}$$

Recognizing that at the instant slip reverses $\hat{\jmath} \cdot v_c(p_c) = 0$, the normal impulse for compression p_c is

$$p_c = k_r\left(r_x + \mu r_y\right)^{-1} M\dot{q}_1(0) \tag{7a}$$

$$= k_r r_c(\sin\theta + \mu\cos\theta)^{-1} M\dot{q}_1(0) \tag{7b}$$

where compression impulse is equivalent to area under the curve of normal component of the contact force *F* as a function of time from incidence until the bristle comes to a stop and begins to rebound. Finally, the work done during compression can be readily evaluated [5] as follows:

$$W_n(p_c) = \int_0^{p_c} v(p)\, dp = -\frac{r_x^2 + \mu r_x r_y}{2k_r^2 M}\, p_c^2 \tag{8}$$

where $v(p) = (r_1/k_r)\,\dot{q}(p)$, and the statement of work done in Eq. (8) during compression is negative to indicate energy is going from the bristle tip to the surface.

During compression, the impulse slows the bristle until all of the kinetic energy of the bristle is transformed to internal energy of deformation and material removal. While some elastic strain energy is released during restitution, when the bristle changes direction and rebounds from the target surface, some energy is dissipated due to plastic deformation. The plastic deformation of the target surface in part causes the residual stresses at the hardened surface.

PRELIMINARY RESULTS AND DISCUSSION

Theoretical Evaluation of Impulsive Load

As shown in the previous section, the compressive impulse due to a single bristle impact with the steel surface can be expressed as,

$$p_c = k_r r_c (\sin\theta + \mu\cos\theta)^{-1} M\dot{q}_1(0) = \frac{k_r^2 M r_c}{(\sin\theta + \mu\cos\theta)}\dot{\theta}(0)$$

whereas the expression for work done during compression is given by:

$$W_n(p_c) = \int_0^{p_c} v(p)\, dp = -\frac{r_x^2 + \mu r_x r_y}{2k_r^2 M}\, p_c^2$$

The work done during compression on the target surface during impact can then be evaluated using known bristle parameters. It has been previously determined in [6] that the mass *M* of a single bristle is 0.001830 lb, and length of 1.063 in. In order to approximate the numerical value of the radius of gyration $k_r^2 = \sqrt{I/M}$, the moment of inertia of a bristle was approximated

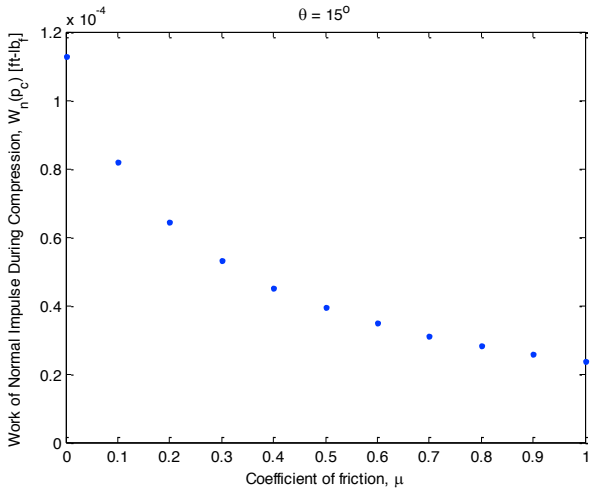

Figure 16: Work of Normal Impulse during compression as a function of friction coefficient

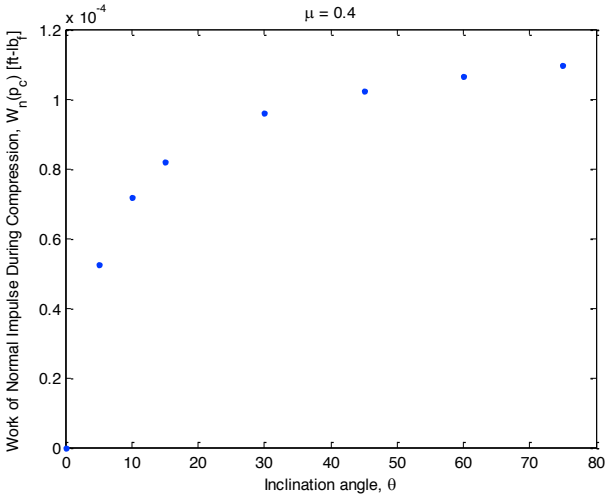

Figure 17: Work of Normal Impulse during compression as a function angle of inclination.

as that of a straight wire, $I = \frac{1}{12} ML^2$. Also, since the hub operates at a speed of approximately 2500 rpm, the initial angular speed $\dot{\theta}(0)$ of the bristle is 261.80 radians per second. Therefore, with the friction coefficient μ and inclination angle θ remaining as the only unknowns, the effect of these parameters can be examined.

The work of the normal impulse during compression was shown to increase as the angle of inclination increases. These results indicate that the bristle tip impacted the target surface at larger inclination angles would result in larger amounts of kinetic energy transferred from bristle to deformation in the target surface. While it is known that some elastic strain energy will be release during restitution in the form of kinetic energy as the bristle changes direction and rebounds from the target surface, some energy is dissipated due to plastic deformation. Therefore, one may conjecture that a greater inclination angle can lead to or promote greater (compressive) residual stresses on and within the target surface.

Conversely, an increase in the friction coefficient also causes the work of normal compression impulse to decrease, indicating that as expected, more energy would be lost to friction forces between the bristle tip and target surface at impact. Since rebound of the bristle tip is desired in order to create the anchor profile, this may suggest that a target surface having very large friction coefficient can decrease the effectiveness of the tool, although the exact limitation of the friction coefficient is not known at this time.

Through-thickness Residual Stress of Bristle Blast Surface

Recently obtained results are shown in Figure 18 for the through-thickness residual stress in ABS-A steel that has been treated via the bristle blasting process. These results indicate that

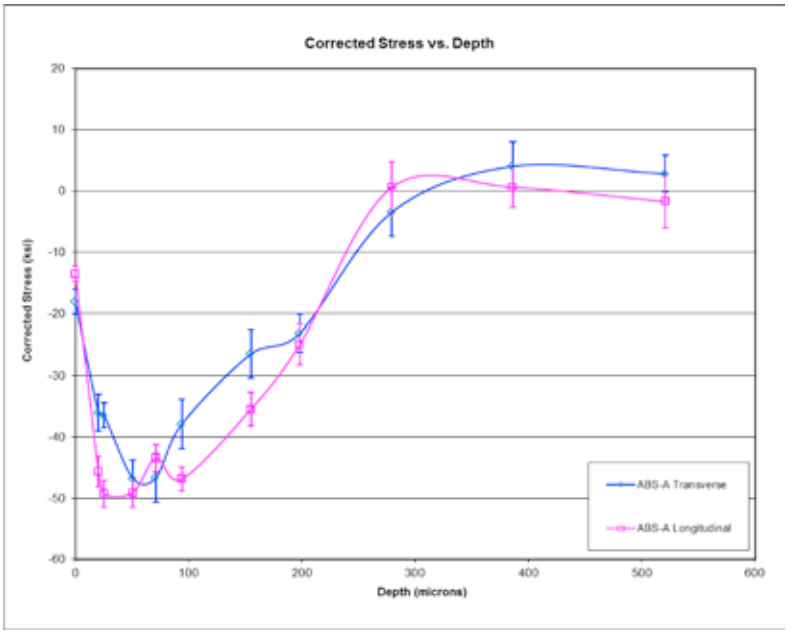

Figure 18 Residual stresses measured using x-ray diffraction of ABS-A bristle blast surface.

significant compressive residual stresses are generated at and below the surface to a depth exceeding 200 microns. Subtle differences of the stress state are obtained when measurement is made along the feed-direction (i.e., along the direction of longitudinal cleaned

rows as shown in Figure 6a, b and c), as opposed to the transverse direction (i.e., perpendicular to the feed direction). The authors are currently engaged in interpreting and identifying additional findings that relate the theoretical impulsive loads generated during impact with the measured tool forces reported in Figure 7.

CONCLUSION

The body of knowledge that has been presented in this paper suggests that bristle blasting is an expedient and thorough process for surface preparation of ABS-A steel. That is, white metal cleanliness (SP-5) and an acceptable anchor profile ($60 \leq Rz \leq 80$) can be readily achieved for a significant duration of steady tool use. Also, preliminary results that have been reported for residual stresses generated during bristle blasting operations indicate that significant compressive residual stresses are generated at and below the surface to a depth exceeding 200 microns. Such a residual stress pattern can represent a significant finding, as it will promote resistance to crack growth, improved fatigue life, and improved resistance to stress corrosion. Finally, precursory modeling and computation has shown that the work done during compression on the target surface during impact is in general agreement with the increased aggressiveness and corresponding forces that are recorded when penetration of the tool is increased during the cleaning process. This area of research merits further investigation, and can provide valuable help in forecasting the behavior of bristle blasting processes.

ACKNOWLEDGMENT

The authors gratefully acknowledge the support and encouragement provided by the project sponsor, Monti Werkzeuge, Bonn, Germany.

REFERENCES

1. Stango, R.J., and Khullar, P., 2009, Recently Developed *Bristle Blasting* Process for Corrosion Removal, 2009 DoD Corrosion Conference, Washington, D.C.
2. Stango, R.J., Fournelle, R. A., Martinez, J. A., and Khullar, P., 2010,Surface Preparation of Ship Construction Steel Via Bristle Blasting Process, NACE Corrosion Conference, San Antonio, TX., 2009, Paper no. 13892.
3. Stango, R.J., 2010, Bristle-blast Surface Preparation Process for Reduced Environmental Contamination and Improved Health/Safety Management, 18th International Oil and Gas Industry and Conference, OSEA, Singapore, November 30-December 3, 2010.
4. Stronge. W.J. “Generalized Impulse and Momentum Applied to Multibody Impact with Friction.” Mechanics of Structures and Machines 29.2 (2001): 239-260.
5. Stronge, W.J. Impact Mechanics. Cambridge University Press. 2000.
6. Khullar, Piyush. “Development & Implementation of Novel Bristle Tool for Surface Treatment of Metallic Components.” Master’s Thesis. Marquette University, 2009.

Art.-Nr.: P-009-03